

Opto-mechanical effect in photoactive nematic main-chain liquid-crystalline elastomers†

Cite this: *Soft Matter*, 2013, **9**, 4621

Antoni Sánchez-Ferrer^{*ab} and Heino Finkelmann^b

Received 10th October 2012
Accepted 21st February 2013

DOI: 10.1039/c3sm27341e

www.rsc.org/softmatter

Monodomains of nematic main-chain liquid-crystalline elastomers containing azoderivatives in the polymer backbone have been studied by means of opto-mechanical experiments at different temperatures for the evaluation of the mechanical response, kinetic rates, activation energies and the isomerization mechanism. The increase in the crosslinking density of the network enhances the light-induced stress in the sample, leading to a better performance and more tunability of the systems when compared to nematic side-chain liquid-crystalline elastomers.

Introduction

Nematic liquid-crystalline elastomers (LCEs) are fascinating materials that combine the rubber elasticity of a common elastomer with the anisotropy of the liquid-crystalline state of order.¹ The local order of the domains in the system is directly connected to the strain imposed on the sample.^{2,3} Main-chain liquid-crystalline elastomers (MCLCEs) are constituted of crosslinked polymer chains containing the mesogens linked through short chains called spacers which directly couple to the polymer backbone.^{4–6}

The local disorder induced by light as an external field, on introducing photoactive molecules as co-monomers that change their chemical structure under irradiation, drives to dimensional changes in the LCE.^{7–10} LCEs have been pointed out as candidates for switchers, actuators or artificial muscles due to their huge change in shape, up to 400%, and the wide range of mechanical properties these materials cover, from kPa to MPa.^{11–18}

Nematic MCLCEs containing azoderivatives as co-monomers have been investigated in order to establish the effect of the crosslinking density on the polymer network, and to compare the mechanical response, kinetics and mechanism of photoisomerization with the same properties of photoactive side-chain liquid-crystalline elastomers (SCLCEs)^{19,20} when light is applied. The change in shape of these azobenzene co-monomers, from the rod-like shape (*trans*-isomer) to the bent-like

shape (*cis*-isomer), leads to an induced local disorder in the surroundings of the molecule and is transmitted through the polymer backbone, inducing a very significant change in the dimensions of the elastomer.

In this paper, we present and discuss new opto-mechanical studies on photoactive nematic MCLCEs together with the effect of the crosslinking degree, and a comparison is made with nematic SCLCEs.

Experimental part

Synthesis of the mesogens and azobenzene derivative

The rod-like mesogens (MCM1 and MCM2)^{21,22} and the azobenzene co-monomer (Azo)¹⁹ were synthesized as described previously. All chemical structures are depicted in Scheme 1.

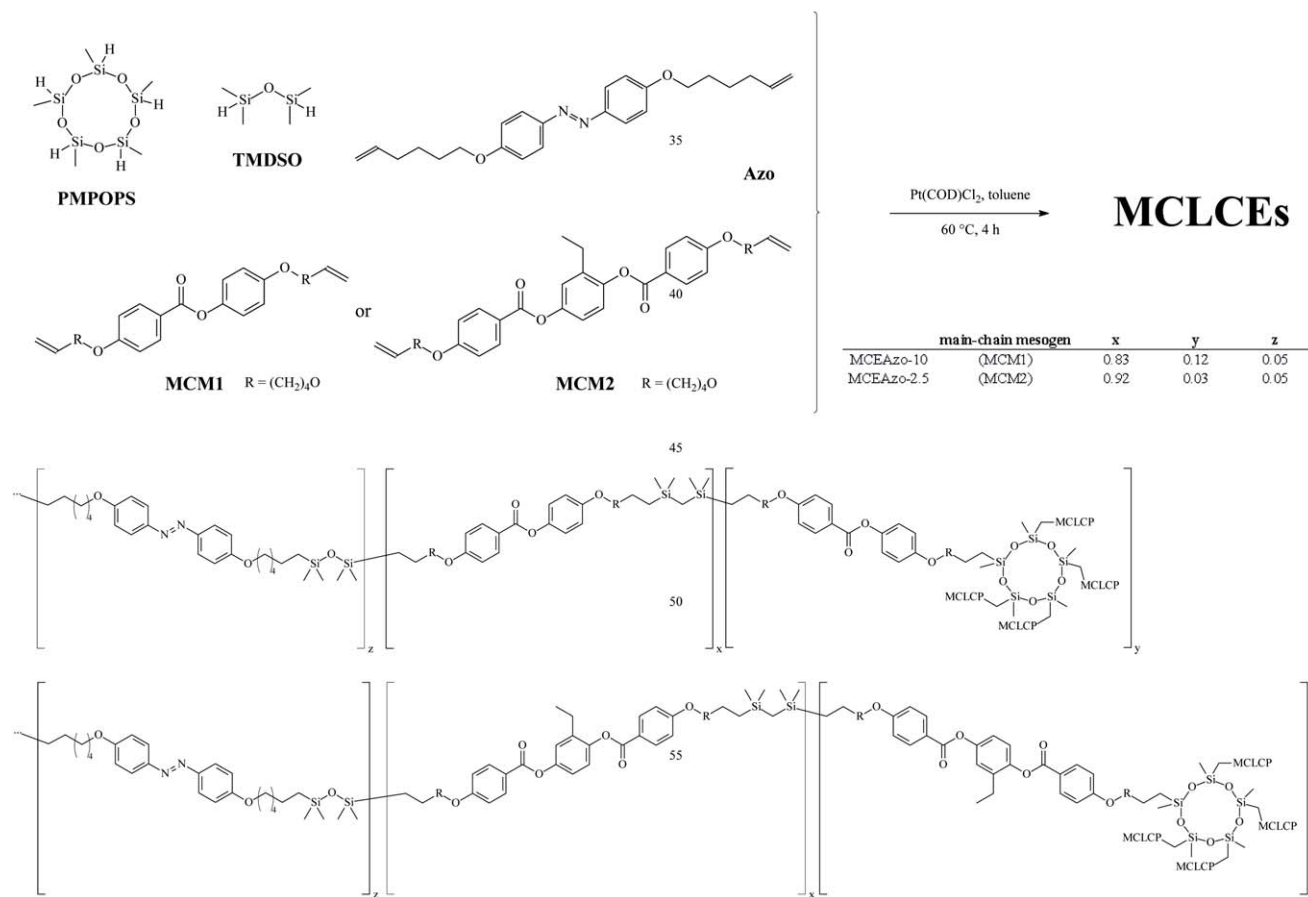
Synthesis of photoactive nematic main-chain liquid-crystalline elastomers

The procedure in the synthesis of MCLCEs was the same as for SCLCEs, but with longer reaction times (4 h). Mixtures of mesogen (MCM1 or MCM2), chain-extender (1,1,3,3-tetramethyldisiloxane, TMDSO), crosslinker (2,4,6,8,10-pentamethyl-1,3,5,7,9,2,4,6,8,10-pentaoxapentasilcane, PMPOPS) and azobenzene co-monomer (Azo) were prepared and partially crosslinked after the non-complete hydrosilylation reaction.²³ The swollen elastomer strip was removed from the spin-casting cell and aligned by applying a strong uniaxial stress and then elongated to uniformly align with the director.²⁴ Then, the unswollen sample was completely cured at 60 °C to fix the monodomain orientation. The composition of these samples was optimized at a level of azobenzene dyes high enough – 5 mol% of the total amount of rod molecules – to see the opto-mechanical effect of the azoderivatives as co-monomers (Scheme 1). At these high concentrations of azobenzene molecules, a nonlinear absorption behavior should be expected, where a photo-bleaching of the dyes together with the

^aETH Zürich, Department of Health Sciences and Technology, Institute of Food, Nutrition & Health, Food & Soft Materials, Schmelzbergstrasse 9, LFO, E29, 8092 Zürich, Switzerland. E-mail: antoni.sanchez@hest.ethz.ch

^bAlbert Ludwigs University, Institute for Macromolecular Chemistry, Stefan-Meier-Str. 31, 79104 Freiburg, Germany

† Electronic supplementary information (ESI) available: Detailed experimental procedures and sample preparation, as well as the analysis of the opto-mechanical experiments at different temperatures and the resulting activation energies, enthalpy and entropy values. See DOI: 10.1039/c3sm27341e



Scheme 1 Synthetic route for the two nematic main-chain liquid-crystalline elastomers: MCEAzo-10 and MCEAzo-2.5.

corresponding increase in the effective transmittance has been suggested to explain the actuation phenomenon in LCs.^{25–27} The final compositions of the two elastomers were the following: MCEAzo-10 : PMPOPS = 5.4 mol%; TMDSO = 40.5 mol%; Azo = 2.7 mol%; MCM1 = 51.4 mol%, and MCEAzo-2.5 : PMPOPS = 1.3 mol%; TMDSO = 47.8 mol%; Azo = 2.5 mol%; MCM2 = 48.4 mol%; all the values are in mol% related to the total amount of monomeric units. The number in the sample's name indicates the molar percentage of cross-linkers with respect to the number of rod molecules.

X-ray measurements showed that these cybotactic nematic samples were well oriented and with values of the order parameter of 0.73 and distances in between mesogenic units of 4.5 Å (see ESI, Fig. S1†).²⁸ The presence of azo compound molecules clearly determines the mechanical and thermal properties of the samples. The two photoactive elastomers have clearing temperatures of 48 and 55 °C for MCEAzo-10 and MCEAzo-2.5, respectively.²⁸ More details on the synthesis and characterization of both MCLCEs are given in the ESI.†

Apparatus and techniques

Opto-mechanical measurements were performed with a self-constructed apparatus designed to measure the retroactive force as a function of time under irradiation, or the relaxation

process in the darkness. In a thermostatted cell controlled using a Haake-F6 thermostat and a Pt100 thermoresistor, the sample was stretched using one Owis SM400 microstep motor and controlled using an Owis LSTEP-12 56.202.0000 microstep controller. The stress (σ) was measured using a Transducer Techniques GS0-10 transducer load cell (10 g) and analysed using a Newport Electronics INFS-1001-DC7 high performance strain gage indicator. All relevant data such as temperature, time and stress (σ) were continuously logged and controlled using National Instruments LabView 7.0 software. The sample was irradiated with UV-light using an Osram XBO150W/1 xenon arc lamp (150 W, 20 V, 7.5 A) that was in a Müller Elektronik-Optik LAX 1530 lamp housing connected to a Müller Elektronik-Optik SVX 1530 power source. To select the right wavelength, a Jobin Yvon H20 UV/Vis/NIR monochromator was used and a Ocean Optics USB2000 UV-Vis spectrophotometer (UV2/OFLV-4 detector, L2 lens, 5 μ m slit, 200–850 nm) connected to the thermostatted cell by a Ocean Optics P400-2-UV/VIS optical fibre (UV/Vis, 2 m, 400 μ m) was attached to the back side of the cell. The temperature of the sample was checked using a Eurotherm Controls 2132 PID temperature controller with a 4–20 mA output loop current limit and a Pt100 linear resistor. The intensity of the radiation reaching the sample was 312 mW cm^{−2}, measured using a calibrated Lot-Oriel Ophir-70260-2 radiant power meter with a Lot-Oriel Ophir-70282 Si-detector

with a PD300-UV head in the range from 250 to 1100 nm, and it was kept constant during the experiments. X-ray scattering experiments were performed using a Philips PW 1730 rotating anode (4 kW) in order to obtain direct information on the SAXS and WAXS reflections in the nematic phases. Cu K α radiation (1.5418 Å) filtered using a graphite monochromator and collimated using a 0.8 mm collimator was used. The incident beam was normal to the surface of the film. The scattered X-ray intensity was detected using a Schneider image plate system (700 × 700 pixels, 250 μ m resolution). Samples were placed in a self-constructed holder where the temperature was controlled using a Haake-F3 thermostat.

Results and discussion

Opto-mechanical experiments

The response under irradiation of nematic photoactive MCLCEs with different crosslinking densities, and with azobenzene derivatives as co-monomers, was investigated with the aim of establishing the effect of the degree of polymerisation or repeating units in the polymer backbone between crosslinking points when light is applied as an external field.

On irradiating the sample, the photoactive azobenzene molecules change their shape from a rod-like shape – *trans*-isomer – which is the most stable isomer form and stabilizes the liquid-crystalline phase, to a bent-like shape – *cis*-isomer – that destabilizes the mesophase. This means that phase transitions of liquid-crystalline systems can be induced isothermally and reversibly by photochemical reactions of photoresponsive guest molecules. This destabilization of the liquid-crystalline phase causes shrinkage in the LCE.^{7–10,19} On stopping the irradiation, the bent-like shaped molecules come back to their original rod-like shape form and, as a consequence, the LCE recovers its original dimensions. This effect is induced by the fact that the *cis*-isomer acts as an impurity for the liquid-crystalline order, and, in the case of MCLCEs, also by the mechanical stress generated by azobenzene present in the polymer backbone. If these photoactive MCLCEs are clamped from both ends of the sample and are irradiated, a retractive force is generated due to the natural length shrinkage, which is not mechanically permitted due to the clamping and thus generates the stress in the sample.

The opto-mechanical response of these two MCLCEs was investigated under a constant pre-load (0.5 g which corresponds to a strain below $\lambda = 1.05$)²⁸ applied on the samples of dimensions 10 mm × 1 mm × 0.250 mm. When irradiated with UV-light at $\lambda = 380$ nm, the *trans*-to-*cis* isomerization caused a decrease of the local order parameter, which could be measured by an increase of the retractive force as a function of time, until the photo-stationary *cis-trans* equilibrium was reached. On reaching this equilibrium state, the irradiation process was stopped and the relaxation *cis*-to-*trans* isomerization process started. These measurements allow the evaluation of the kinetics of the isomerisation process.

In a previous communication,¹⁹ both the *trans*-to-*cis* photo-isomerization and the *cis*-to-*trans* thermal-isomerization were described as a stretched exponential growth and a stretched exponential decay, respectively. The lifetime related to the

photo-isomerization of the azo compounds is related to both the photo-isomerization (k_1) and the thermal-isomerization (k_2) processes, $\tau_{\text{photo}} = (k_1 + k_2)^{-1} = k_{\text{photo}}^{-1}$, and the curve which describes the irradiation of the sample has the following expression:

$$\Delta\sigma(t) = \Delta\sigma_{\text{max}} \left(1 - \exp\left(\frac{-(t - t_0)}{\tau_{\text{photo}}}\right)^{\beta_{\text{photo}}}\right) + \Delta\sigma_0 \quad (1)$$

where $\Delta\sigma_{\text{max}}$ is the maximum mechanical response, $\Delta\sigma_0$ is the applied pre-load, and β_{photo} is the exponential factor.

The lifetime corresponding to the relaxation of the network in the darkness only depends on the thermal-isomerization (k_2) process, $\tau_{\text{thermal}} = (k_2)^{-1} = k_{\text{thermal}}^{-1}$, and the curve which follows this decay is:

$$\Delta\sigma(t) = \Delta\sigma_{\text{max}} \exp\left(\frac{-(t - t_0)}{\tau_{\text{thermal}}}\right)^{\beta_{\text{thermal}}} + \Delta\sigma_0 \quad (2)$$

where $\Delta\sigma_{\text{max}}$ is the starting maximum mechanical response, $\Delta\sigma_0$ is the initially applied pre-load, and β_{thermal} is the corresponding exponential factor.

The corresponding opto-mechanical experiments showed the behaviour of the stress ($\Delta\sigma$) as a function of time (Fig. 1a),

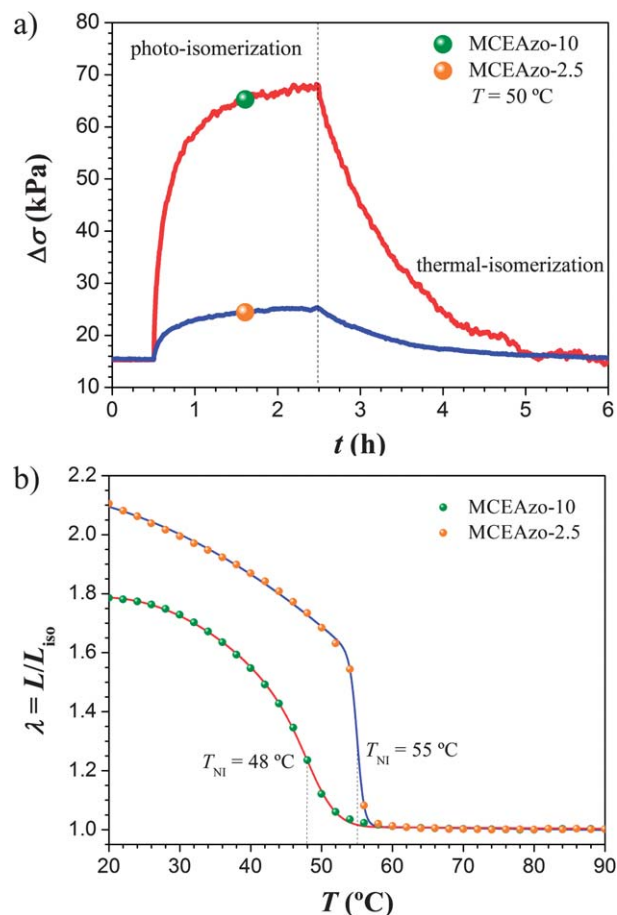


Fig. 1 (a) Opto-mechanical experiment at 50 °C on the samples MCEAzo-10 and MCEAzo-2.5 at $\lambda = 380$ nm. (b) Uniaxial thermal expansion ($\lambda = L/L_{\text{iso}}$) as a function of temperature for the two nematic MCLCEs. Note: both experiments were performed under a constant pre-load of $F = 0.5$ g.

where the two isomerization processes are presented for both MCLCE samples. The samples' change in dimensions was taken into consideration.¹⁹ Fig. 1b shows the uniaxial thermal expansion of both samples, where the maximum length ratio λ at 20 °C is related to the crosslinking density and the inflexion point of each curve to the nematic-to-isotropic temperature T_{NI} . Thus, samples with low crosslinking density expand/contract more than those with high crosslinking density. The clearing temperature for the 10 mol% crosslinking density sample (MCEAzo-10) is lower than the isotropization temperature of the 2.5 mol% crosslinked sample (MCEAzo-2.5) due to the fact that the isotropic crosslinker acts as an impurity, introducing some disorder and lowering the transition temperature.²⁹

From the analysis of the opto-mechanical experiments at different temperatures, an important effect can be seen, coming from the chemical constitution of the polymer network: an increase of 4 times the crosslinking density in the sample MCEAzo-10 with respect to the sample MCEAzo-2.5 shows a mechanical response which is 8 times higher at low temperatures (30 °C), but almost the same at high temperatures (70 °C) (Fig. 2). Moreover, at a low temperature (45 °C), where the

maximum response is observed for all systems, the most responsive nematic main-chain system (MCEAzo-10) is up to 2 times more efficient than the best of the side-chain networks with an azobenzene derivative as the crosslinker (SCEAzo2-c-10), and the less crosslinked main-chain system (MCEAzo-2.5) is 30% more responsive than the worst of the side-chain elastomers containing a flexible pendant azobenzene molecule (SCEAzo4-p-10).¹⁹ For the two crosslinking compositions in the main-chain elastomers, the samples have 4 (MCEAzo-10) and 16 (MCEAzo-2.5) main-chain repeating units between two crosslinking points which correspond to distances of 11 and 48 nm, respectively (the data are obtained from the evaluation of X-ray measurements; see ESI, Fig. S1†). These lengths are much longer than the corresponding lengths of SCLCEs with contour lengths around 3 nm for the polysiloxane backbone which consists of 8 side-chain mesogens between crosslinking points. Thus, the nature of the polymer backbone – anisotropic rod-containing MCLCEs or isotropic flexible polymer backbone SCLCEs – and the degree of crosslinking have a huge effect on the mechanical response in LCEs.

The opto-mechanical experiments have been performed at different temperatures in order to identify the activation energy for both the photo- and back-isomerization processes. By fitting these curves at different temperatures, the maximum stress ($\Delta\sigma_{\max}$), kinetics constants (k_1 and k_2) and the exponential factors (β_{photo} and β_{thermal}) for both processes can be calculated (see ESI, Tables S1 and S2†). In Fig. 3, the normalized mechanical responses ($\Delta\sigma$) are shown as a function of time, under irradiation and in the darkness, at different temperatures, for both samples MCEAzo-10 and MCEAzo-2.5. For the calculation of normalized curves during the photo- and the thermal-isomerization processes, the following expression was used: $\Delta\sigma_{\text{norm}} = [\Delta\sigma(t) - \Delta\sigma_0]/\Delta\sigma_{\max}$, where $\Delta\sigma(t)$ is the mechanical response at a certain time, $\Delta\sigma_0$ is the applied pre-stress, and $\Delta\sigma_{\max}$ is the maximum mechanical response. The values of the exponential factors depend strongly on the studied isomerization process. Thus, during irradiation the exponential factor is $\beta_{\text{photo}} \approx 0.55$ raising up to 0.70 at high temperatures, while during the relaxation process the exponential factor is $\beta_{\text{thermal}} \approx 1$ (Table 1), which indicates that the photo-isomerization process deviates from the ideal exponential behaviour observed in the thermal-isomerization process in main-chain elastomers, and from the values of the side-chain systems ($\beta_{\text{photo}} \approx 0.70\text{--}0.80$).¹⁹ This effect can be explained by considering the effective stress transmission through the whole macromolecule in MCLCEs: the azobenzene co-monomer not only induces disorder due to the change in molecular shape from *trans* to *cis*, it creates an extra mechanical response which stretches the polymer chain and brings the crosslinking points closer: the so-called cooperative effect. The mechanical responses of both main-chain elastomeric samples, and all previous side-chain elastomers, do not show a maximum in the vicinity of the clearing temperature, as predicted by the published literature,⁹ and the mechanical response is higher at low temperatures.

Only a pronounced decay as a function of temperature was noticed for the elastomers with azobenzene crosslinkers, and a slight decay with a small local maximum in the case of the

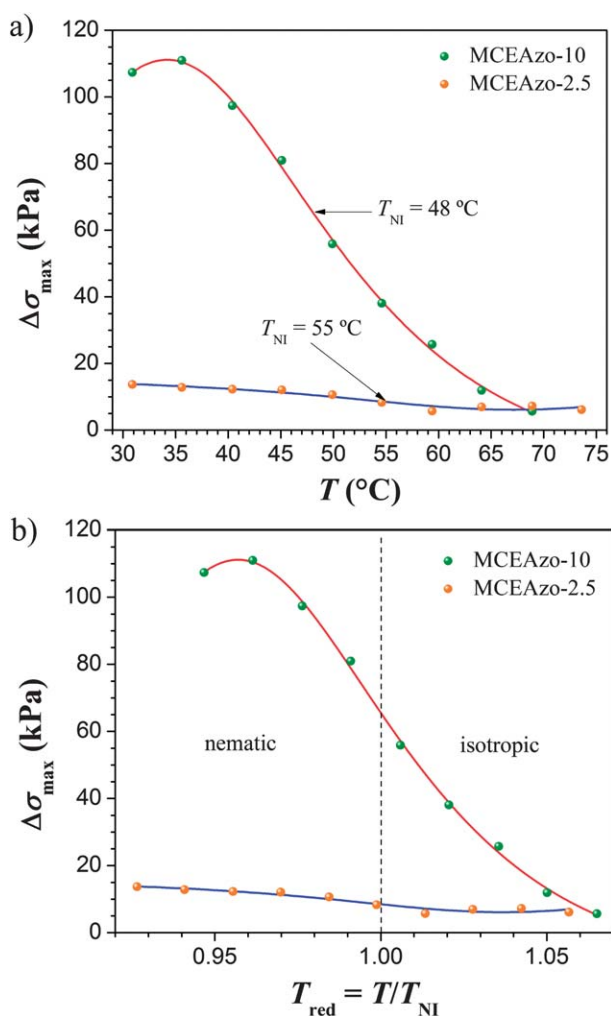


Fig. 2 Maximum response ($\Delta\sigma_{\max}$) for the two MCLCEs (a) as a function of temperature, and (b) as a function of the reduced temperature.

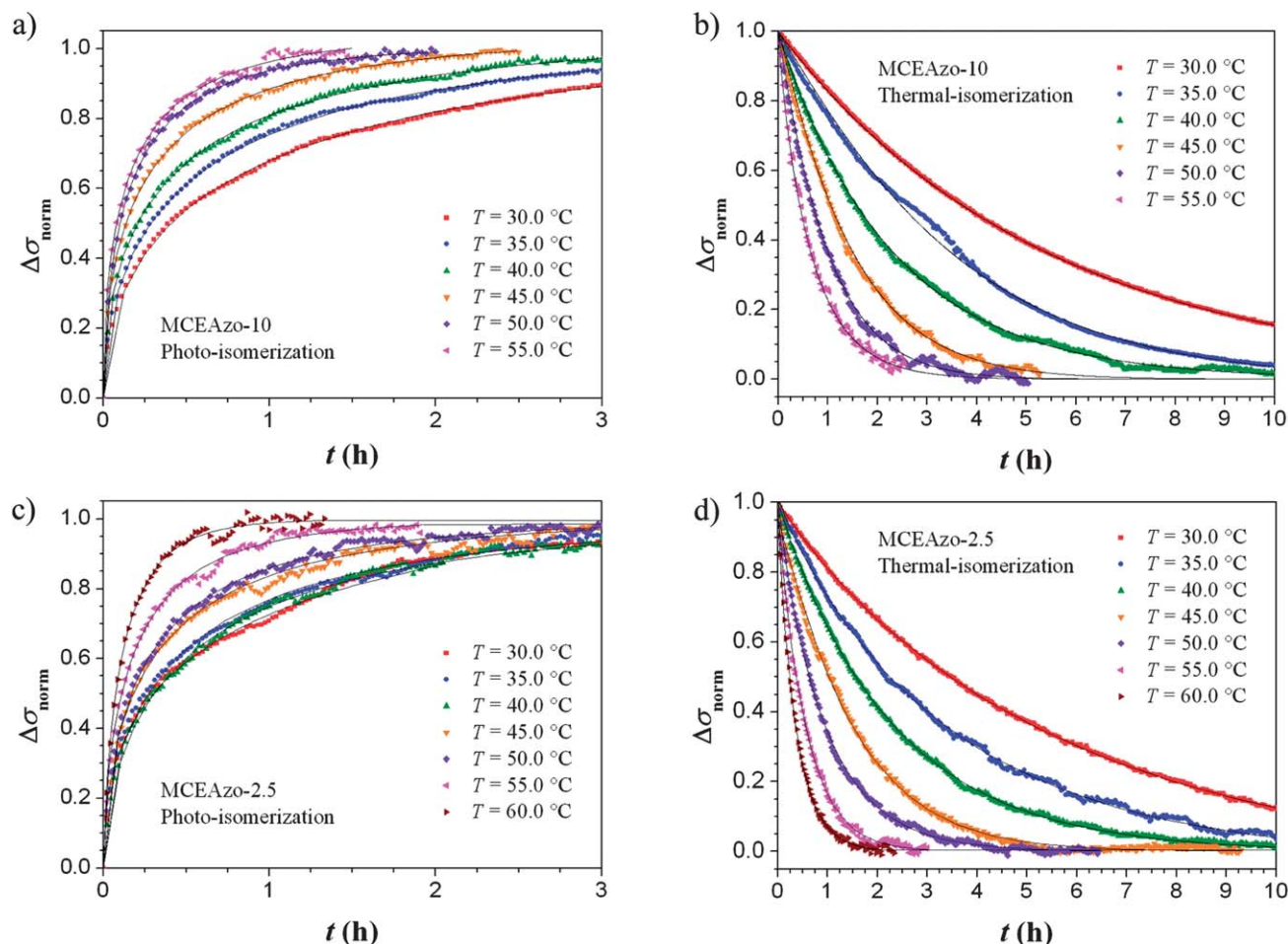


Fig. 3 Normalized (a) photo-isomerization curves and (b) thermal-isomerization curves for the sample MCEAzo-10, and normalized (c) photo-isomerization curves and (d) thermal-isomerization curves for the sample MCEAzo-2.5 at different temperatures. Note: for the normalized photo- and thermal-isomerization curves, the following definition was used: $\Delta\sigma_{\text{norm}} = [\Delta\sigma(t) - \Delta\sigma_0] / \Delta\sigma_{\text{max}}$.

Table 1 Exponential factors during the photo-isomerization (β_{photo}), and the thermal-isomerization (β_{thermal}) processes, and their corresponding activation energies (E_a) and half-life times ($t_{1/2}$) at 50 °C for each sample

| Sample | β_{photo} | E_a (kJ mol ⁻¹) | $t_{1/2}$ (h) | β_{thermal} | E_a (kJ mol ⁻¹) | $t_{1/2}$ (h) |
|------------|------------------------|----------------------------------|---------------|--------------------------|----------------------------------|---------------|
| MCEAzo-10 | 0.587 | 63 | 0.13 | 1.000 | 71 | 0.68 |
| MCEAzo-2.5 | 0.580 | 36 | 0.22 | 0.955 | 77 | 0.65 |

pendant groups. That can be explained by the *trans*-to-*cis* isomerization affecting T_{NI} , but not the order. These azobenzene crosslinkers have a higher mechanical effect than the disorder generated by the *cis*-isomer in the LC matrix. Another relevant fact is that all samples are more responsive at low temperatures, where the Young's modulus is higher when approaching T_g .^{19,24}

Photo-isomerization and thermal-isomerization: kinetics and activation energy

The information on the kinetics of photo- and thermal-isomerization can be evaluated by fitting the curves of each opto-

mechanical experiment at different temperatures. The kinetic constants and the *cis*-isomer populations were determined using the corresponding lifetimes τ_1 and τ_2 , $\phi_{\text{cis}} = (\tau_2 - \tau_1) / \tau_2$ (see ESI, Table S3†).

The relationship between the rate of a reaction and its temperature is quantitatively determined by the Arrhenius equation $k = A\exp(-E_a/RT)$, where k is the kinetic constant, A is the pre-exponential factor, E_a is the activation energy, R is the universal gas constant, and T is the temperature (see ESI, Fig. S2†). The activation energies and half-life times are summarised in Table 1 for both photoactive MCLCEs.

The activation energy in the photo-isomerization process depends on the nature of the azobenzene compound,^{19,30} as well as on the nature of the studied macromolecule. The values obtained for the activation energies during the photo-isomerization process differ from one sample to the other. The highly crosslinked elastomer (MCEAzo-10) has an energetic barrier of 63 kJ mol⁻¹, much higher than the value for the low crosslinked system (MCEAzo-2.5) of 36 kJ mol⁻¹ (Table 1), which does not differ that much from those in side-chain elastomers.¹⁹ The explanation recalls the idea of the stress-avoiding isomerization due to the short length and rigidity of the polymer backbone

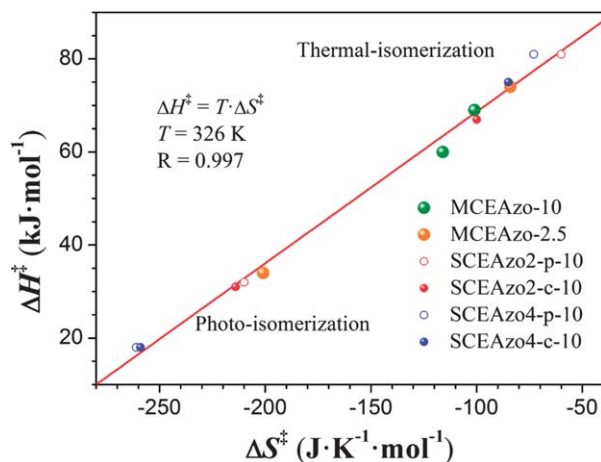


Fig. 4 Activation enthalpy (ΔH^\ddagger) versus activation entropy (ΔS^\ddagger) of the *trans*-to-*cis* photo-isomerization and *cis*-to-*trans* thermal-isomerization processes for the two photoactive nematic MCLCEs, and the four photoactive nematic SCLCEs from ref. 19.

which acts as a spring between crosslinking points, delaying the photo-isomerization process for the highly crosslinked main-chain elastomer.

In the thermal-isomerization process, both samples have similar energetic barriers, 71 kJ mol^{-1} and 77 kJ mol^{-1} (Table 1). The network helping the recovery of the original *trans*-state, which is easier for the sample with a shorter polymer backbone, explains this difference in the activation energy. The values obtained from the Eyring equation $k = k_B T / h \exp(-\Delta H^\ddagger / RT) \exp(\Delta S^\ddagger / R)$ are in agreement with those from the Arrhenius equation. Thus endothermic processes ($\Delta H^\ddagger > 0$), and ordered intermediates ($\Delta S^\ddagger < 0$) suggest a more organized transition state, where more negative entropy values lead to lower enthalpy needs (see ESI, Table S4†). The enthalpy and entropy values for the two photoactive nematic MCLCEs during both photo- and thermal-isomerization processes fall on the same curve (Fig. 4) as nematic SCLCEs, and low molecular-mass liquid crystals.^{19,31} That is a clear indication that both isomerization processes follow the same inversion mechanism or isokinetic relationship during the *trans*-to-*cis* and *cis*-to-*trans* isomerization.³²

Conclusions

The opto-mechanical response of new photosensitive nematic main-chain liquid-crystalline elastomers (MCLCEs) with different crosslinking densities has been studied, and compared to their analogous side-chain systems. It has been shown that by increasing the crosslinking density – by shortening the polymer length between crosslinking points – the elastomer becomes more responsive than its corresponding low crosslinked partner, or than side-chain systems with a similar crosslinking density. No maximum in the mechanical response in the vicinity of the clearing temperature has been observed, and the mechanical response is maximal at low temperatures due to the high elastic modulus of the samples, and better *cis*-isomer conversion.

The pure photo-isomerization and thermal-isomerization processes have been studied at different temperatures, and the kinetic constants for both processes, as well as the energetic barriers, have been evaluated. The results show a slower response for the highly crosslinked system, due to the stress-avoiding isomerization effect related to the short polymer backbone between crosslinking points. The evaluation of the energies involved in these isomerisation processes shows that MCLCEs strongly affect the photo-isomerization of the azobenzene compound, making the process more difficult for a more crosslinked network.

Finally, the isomerization mechanism for MCLCEs involved in both processes is the same as for SCLCEs: the inversion mechanism. In this isomerization mechanism where an inversion through a linear state takes place, a more ordered transition state (decreased entropy) has less energetic demands (decreased enthalpy).

Acknowledgements

The authors acknowledge financial support from the Research Training Networks FUNCTIONAL LIQUID-CRYSTALLINE ELASTOMERS (FULCE-HPRNCT-2002-00169) and Fonds der Chemischen Industrie.

References

- 1 M. Warner and E. M. Terentjev, *Liquid Crystal Elastomers*, Clarendon, Oxford, 2007, (revised edition).
- 2 H. R. Brand, H. Pleiner and P. Martinoty, *Soft Matter*, 2006, **2**, 182.
- 3 D. L. Thomsen, P. Keller, J. Naciri, R. Pink, H. Jeon, D. Shenoy and B. R. Ratna, *Macromolecules*, 2001, **34**, 5868.
- 4 B. Donnio, H. Wermter and H. Finkelmann, *Macromolecules*, 2000, **33**, 7724.
- 5 H. Wermter and H. Finkelmann, *e-Polym.*, 2001, **013**, 1.
- 6 A. R. Tajbakhsh and E. M. Terentjev, *Eur. Phys. J. E: Soft Matter Biol. Phys.*, 2001, **6**, 181.
- 7 H. Finkelmann, E. Nishikawa, G. G. Pereira and M. Warner, *Phys. Rev. Lett.*, 2001, **87**, 015501.
- 8 P. M. Hogan, A. R. Tajbakhsh and E. M. Terentjev, *Phys. Rev. E: Stat., Nonlinear, Soft Matter Phys.*, 2002, **65**, 041720.
- 9 J. Cviklinski, A. R. Tajbakhsh and E. M. Terentjev, *Eur. Phys. J. E: Soft Matter Biol. Phys.*, 2002, **9**, 427.
- 10 C. L. M. Harvey and E. M. Terentjev, *Eur. Phys. J. E: Soft Matter Biol. Phys.*, 2007, **23**, 185.
- 11 H. Finkelmann, S. T. Kim, A. Muñoz, P. Palfy-Muhoray and B. Taheri, *Adv. Mater.*, 2001, **13**, 1069.
- 12 G. H. E. Bergmann, H. Finkelmann, V. Percec and M. Zhao, *Macromol. Rapid Commun.*, 1997, **18**, 353.
- 13 D. K. Shenoy, D. L. Thomsen, A. Srinivasan, P. Keller and B. R. Ratna, *Sens. Actuators, A*, 2002, **96**, 184.
- 14 S. Courty, J. Mine, A. R. Tajbakhsh and E. M. Terentjev, *Europhys. Lett.*, 2003, **64**, 654.
- 15 M. Chambers, B. Zalar, M. Remškar, S. Žumer and H. Finkelmann, *Appl. Phys. Lett.*, 2006, **89**, 243116.

- 16 T. Fischl, A. Albrecht, H. Wurmus, M. Hoffmann, M. Stubenrauch and A. Sánchez-Ferrer, *Kunststoffe*, 2006, **96**, 30.
- 17 A. Sánchez-Ferrer, T. Fischl, M. Stubenrauch, H. Wurmus, M. Hoffmann and H. Finkelmann, *Macromol. Chem. Phys.*, 2009, **210**, 1671.
- 18 A. Sánchez-Ferrer, T. Fischl, M. Stubenrauch, A. Albrecht, H. Wurmus, M. Hoffmann and H. Finkelmann, *Adv. Mater.*, 2011, **23**, 4526.
- 19 A. Sánchez-Ferrer, A. Merekalov and H. Finkelmann, *Macromol. Rapid Commun.*, 2011, **32**, 672.
- 20 A. Sánchez-Ferrer, *Proc. SPIE*, 2011, **8107**, 810702.
- 21 A. Sánchez-Ferrer and H. Finkelmann, *Macromolecules*, 2008, **41**, 970–980.
- 22 S. Krause, R. Dersch, J. H. Wendorff and H. Finkelmann, *Macromol. Rapid Commun.*, 2007, **28**, 2062.
- 23 B. Marciniec, *Comprehensive Handbook on Hydrosilylation*, Pergamon, Oxford, 1992.
- 24 H. Finkelmann, A. Greve and M. Warner, *Eur. Phys. J. E: Soft Matter Biol. Phys.*, 2001, **5**, 281.
- 25 D. Corbett and M. Warner, *Phys. Rev. Lett.*, 2007, **99**, 174302.
- 26 D. Corbett, C. L. van Oosten and M. Warner, *Phys. Rev. A: At., Mol., Opt. Phys.*, 2008, **78**, 013823.
- 27 D. Corbett and M. Warner, *Phys. Rev. E: Stat., Nonlinear, Soft Matter Phys.*, 2008, **77**, 051710.
- 28 A. Sánchez-Ferrer and H. Finkelmann, *Mol. Cryst. Liq. Cryst.*, 2009, **508**, 348.
- 29 A. Lebar, Z. Kutnjak, S. Žumer, H. Finkelmann, A. Sánchez-Ferrer and B. Zalar, *Phys. Rev. Lett.*, 2005, **94**, 197801.
- 30 J. Garcia-Amorós, A. Sánchez-Ferrer, W. A. Massad, S. Nonell and D. Velasco, *Phys. Chem. Chem. Phys.*, 2010, **12**, 13238.
- 31 J. Garcia-Amorós, M. Martínez, H. Finkelmann and D. Velasco, *J. Phys. Chem. B*, 2010, **114**, 1287.
- 32 I. Favier, M. Gómez, J. Granell, M. Martínez, M. Font-Bardía and X. Solans, *Dalton Trans.*, 2005, 123.